Journal of Sustainable Mining 18 (2019) 287–296

Contents lists available at ScienceDirect

Journal of Sustainable Mining

journal homepage: www.elsevier.com/locate/jsm

Research paper

Soft computing-based technique as a predictive tool to estimate blast-induced ground vibration

Clement Kweku Arthur[a], Victor Amoako Temeng[a,*], Yao Yevenyo Ziggah[b]

[a] Mining Engineering Department, Faculty of Mineral Resources Technology, University of Mines and Technology, Tarkwa, Western Region, Ghana
[b] Geomatic Engineering Department, Faculty of Mineral Resources Technology, University of Mines and Technology, Tarkwa, Western Region, Ghana

ARTICLE INFO

Keywords:
Radial basis function neural network
Back propagation neural network
Generalised regression neural network
Wavelet neural network
Group method of data handling
Ground vibration

ABSTRACT

The safety of workers, the environment and the communities surrounding a mine are primary concerns for the mining industry. Therefore, implementing a blast-induced ground vibration monitoring system to monitor the vibrations emitted due to blasting operations is a logical approach that addresses these concerns. Empirical and soft computing models have been proposed to estimate blast-induced ground vibrations. This paper tests the efficiency of the Wavelet Neural Network (WNN). The motive is to ascertain whether the WNN can be used as an alternative to other widely used techniques. For the purpose of comparison, four empirical techniques (the Indian Standard, the United State Bureau of Mines, Ambrasey-Hendron, and Langefors and Kilhstrom) and four standard artificial neural networks of backpropagation (BPNN), radial basis (RBFNN), generalised regression (GRNN) and the group method of data handling (GMDH) were employed. According to the results obtained from the testing dataset, the WNN with a single hidden layer and three wavelons produced highly satisfactory and comparable results to the benchmark methods of BPNN and RBFNN. This was revealed in the statistical results where the tested WNN had minor deviations of approximately 0.0024 mm/s, 0.0035 mm/s, 0.0043 mm/s, 0.0099 and 0.0168 from the best performing model of BPNN when statistical indicators of Mean Absolute Error (MAE), Root Mean Square Error (RMSE), Relative Root Mean Square Error (RRMSE), Correlation Coefficient (R) and Coefficient of determination (R^2) were considered.

1. Introduction

Mining, which is the extraction of any naturally occurring mineral substance: solid, liquid and gas from the earth, has been a human activity since pre-historic times. Through mining, all metals needed by humans have been made available. Mining in its broader sense has been found to consist of five different stages, namely: prospecting, exploration, development, exploitation and reclamation. The exploitation stage employs drilling and blasting to break the in-situ rock mass into smaller fragments so as to be easily loaded and hauled for processing. Blasting, however, results in many unwanted effects due to the wastage of the energy produced during the detonation of explosives (Tripathy, Shirke, & Kudale, 2016). These unwanted effects include: ground vibration, air overpressure, back-break, over-break, flyrock and air pollution. This study is focused on ground vibration.

After the initiation of each blast, high pressure gases are created which crush the adjacent walls of the blast-hole. Compressive and tensile stress waves are then produced from the blastholes in radial directions to further break the in-situ rock mass. Some of the high energy released to fragment the in-situ rock mass propagates through the ground as seismic waves with varying frequencies. The movement of these seismic waves through the ground as a result of the detonation of explosives in a blast-hole is what is referred to as ground vibration.

Ground vibration is characterised by peak particle velocity (PPV) and usually measured in millimetres per second (mm/s) (Rustan, Cunningham, Fourney, Simha, & Spathis, 2010). However, ground vibration induced by blasting is of great concern to mining and civil industries because, when proper caution is not taken, it can adversely affect the environment when the levels of intensity are high. This may even lead to the closure of operations. Several pieces of research (Armstrong, 2001; Stojadinovic, Zikic, & Pantovic, 2011; Silva-Castro, 2012 and references therein) have been conducted to explain this complex phenomenon and the causative factors that lead to their level of intensity.

In relation to explaining real life complex situations, scholars over the years have adapted to the use of mathematical models, which rely on interrelationship between parameters that have been found to lead to the occurrence of real-world situations. Thus, in the study of ground

* Corresponding author.
E-mail address: vatemeng@umat.edu.gh (V.A. Temeng).

https://doi.org/10.1016/j.jsm.2019.10.001
Received 29 June 2019; Received in revised form 29 August 2019; Accepted 24 October 2019
Available online 26 November 2019

vibration induced by blasting, many empirical models (e.g. the United State Bureau of Mines (USBM) model, the Indian Standard model, the Langefors and Kihlstrom model and the Ghosh and Daemen and Ambraseys and Hendron model) solely based on distance from the monitoring station and blasting point, and the maximum charge per delay have been developed (Rai & Singh, 2004; Langefors & Kihlstrom, 1963; Gupta, Roy, & Singh, 1987; Ghosh & Daemen, 1983; Ambraseys & Hendron, 1968; Indian Standard Institute, 1973; Roy, 1991; Davies, Farmer, & Attewell, 1964; Duvall & Petkof, 1959). These techniques are heavily applied in almost all mining and civil engineering companies in order to monitor and predict ground vibration induced by blasting. Their frequent use is due to their simplicity of application. However, studies such as (Khandelwal & Singh, 2009; Parida & Mishra, 2015; Ragam & Nimaje, 2018a; Saadat, Khandelwal, & Monjezi, 2014) have revealed the inability of empirical techniques to predict ground vibration induced by blasting accurately. Authors, for example, Khandelwal & Singh, 2009, and Ghasemi, Ataei, and Hashemolhosseini (2013) have attributed poor performance to their failure to take into account other effective blasting parameters, such as hole depth, hole diameter, burden, bench height, stemming length, spacing, total charge, powder factor, number of holes and rock mass strength that all contribute to the generation of the ground vibration induced by blasting. Moreover, the interactions between these effective parameters are very complicated, therefore, making blast-induced ground vibration a highly complex phenomenon to model (Dehghani & Ataee-pour, 2011).

These realisations have increased the need for testing new techniques that can provide reliable, efficient and accurate prediction results to serve the mining and civil engineering industries. This necessity has led to the application of the Artificial Neural Network (ANN) which has been found to address the complex nature of ground vibration and overcome the weaknesses in the empirical techniques, as ANN has the ability to model complex nonlinear systems. Additionally, due to its input-output mapping and adaptive capabilities, it can easily learn the underlying relationship between the many interrelated effective parameters and the ground vibration. This makes ANN efficient at predicting the outputs of new inputs when trained. A review of previous studies has shown that the Back Propagation Neural Network (BPNN) has been extensively applied to predict blast-induced ground vibration (Khandelwal & Singh, 2006; Khandelwal & Singh, 2007; Khandelwal & Singh, 2009; Amnieh, Mozdianfard, & Siamaki, 2010; Monjezi, Ahmadi, Sheikhan, Bahrami, & Salimi, 2010; Monjezi, Ghafurikalajahi, & Bahrami, 2011; Dehghani & Ataee-pour, 2011; Mohamad, Noorani, Armaghani, & Saad, 2012; Monjezi, Hasanipanah, & Khandelwal, 2013; Xue & Yang, 2014; Saadat et al., 2014; Álvarez-Vigil, González-Nicieza, López Gayarre, & Álvarez-Fernández, 2012; Görgülü et al., 2013; Lapčević, Kostić, Pantović, & Vasović, 2014; Görgülü et al., 2015; Shahri & Asheghi, 2018; Iramina et al., 2018; Ragam & Nimaje, 2018a). Only a few studies have been conducted using the radial basis function neural network (RBFNN) and the generalised regression neural network (GRNN)for blast-induced ground vibration prediction (Monjezi et al., 2010; Xue & Yang, 2014; Ragam, & Nimaje, 2018b, 2018c). Moreover, the Group Method of Data Handling (GMDH) technique which is an extension of the artificial neural network has only been applied in the literature by Mokfi, Shahnazar, Bakhshayeshi, I., Derakhsh, and Tabrizi (2018) to predict blast-induced ground vibration. Other methods that have been developed by researchers in recent times for the prediction of ground vibration induced by blasting include: support vector machine (SVM), adaptive neuro-fuzzy inference systems (ANFIS), classification and regression tree (CART), rock engineering systems and hybrid intelligent models, where metaheuristic algorithms such as gene expression programming, genetic programming and particle swarm optimisation are used to optimise artificial intelligent methods (Hajihassani, Armaghani, Marto, & Mohamad, 2015; Armaghani et al., 2015a, 2016; Hasanipanah, Monjezi, Shahnazar, Armaghani, & Farazmand, 2015; Armaghani, Momeni, Abad, & Khandelwal, 2015b; Faradonbeh et al., 2016a; Monjezi, Baghestani, Faradonbeh, Saghand, & Armaghani, 2016; Ghoraba, Monjezi, Talebi, Armaghani, & Moghaddam, 2016; Faradonbeh, Armaghani, Monjezi, & Mohamad, 2016b; Hasanipanah, Faradonbeh, Amnieh, Armaghani, & Monjezi, 2017a; Hasanipanah, Golzar, Larki, Maryaki, & Ghahremanians, 2017b; Hasanipanah, Naderi, Kashir, Noorani, & Qaleh, 2017c; Shahnazar et al., 2017; Taheri, Hasanipanah, Golzar, & Majid, 2017; Hasanipanah, Armaghani, Amnieh, Koopialipoor, & Arab, 2018; Armaghani, Hasanipanah, Amnieh, & Mohamad, 2018). The conclusions made in these studies revealed that ANN (BPNN, RBFNN, GRNN and GMDH) and the other aforementioned soft computing methods can be used to predict ground vibration induced by blasting accurately.

Despite the widespread use of ANN as presented, BPNN has only been applied to one mine in Ghana to predict ground vibration induced by blasting (Tiile, 2016). With the growing popularity and interest in ANN methods in mining sciences coupled with the advancement of soft computing techniques, the authors believe that it will be an excellent opportunity to test new alternative prediction tools. This study therefore applied the wavelet neural network (WNN) to ascertain its efficiency as a reliable alternative technique to the widely used ANN methods. The motivation for applying WNN was based on its global optimum realisation, higher generalisation performance and good computational efficiency, as reported in the literature. These characteristics enable WNN to adapt to data sets appropriately. The derived computational benefits from WNN can be confirmed in a number of studies found in geosciences (see e.g. Fengqi & Lijuan, 2015; Ghasemi & Ghorbani, 2007; Hung, Huang, & Wen, 2004; Okkan, 2012; Ramana, Krishna, Kumar, & Pandey, 2013; Wang & Ding, 2003; Yue & Shaohong, 2014; Zhou, Wang, Wang, & Yin, 2016). The accuracy and reliability of the WNN approach was compared with the widely used BPNN, RBFNN, GRNN, GMDH and conventional empirical models of USBM, Ambrasey-Hendron, Indian Standard and Langefors-Kihlstrom.

The remaining sections of this paper consist of the following: information about the study site and description of the data are presented in Section 2. Section 3 contains a concise description of the various approaches employed in this study. Section 4 contains a description of the model performance indices used to evaluate the accuracy of the developed models. Section 5contains the results obtained and the discussions of this study. The study concludes with Section 6.

2. Description of the study site and dataset

This study was carried out in a manganese open pit mine situated in Tarkwa, Ghana. The study site lies geographically between longitude 1° 59′ W and latitude 5° 16′ N of the Wassa West Municipality in the Western Region of Ghana. The Mine is approximately a 304 km drive from Accra (Ghana's capital) and approximately a 63 km drive from the regional capital, Takoradi (Amegbey & Afum, 2015). The location of the study area is shown in Fig. 1.

The Mine operates three pits, which are: pits E, F and G. Pit G has been subdivided into G North (GN); G South East (GSE); G South West (GSW); G Central East (GCE) and G Central West (GCW). It is worth mentioning that, currently, active mining is taking place in pit G. The mine is characterised by three main types of rock formations namely: Metatuffs, Manganiferous horizon and Greenstones. The mine uses Sandvik Pantera DP1500i drill rigs, Volvo AD35 and O & K excavators, CAT 777F and Komatsu HD 465 rear dump trucks for drilling, loading and hauling purposes, respectively. Blasting of the in-situ rock mass is done through the use of Emulsion RIOMEX 7000 as the main explosive material. Priming of drilled holes is done using a 500 ms down the hole detonator and a 250 g Pentolite booster with either a 25 ms or 42 ms non-electric dual delay detonator. Furthermore, the surface connectors have delay times of 17, 42 and 67 ms. The Mine applies a nonelectric blasting system and detonating cord for initiation. A stemming length of 3 m is adopted and a blend of 15 mm and 20 mm sized gravels are used as stemming material. This is done to ensure proper confinement. The drilled holes have a diameter of 115 mm, an average depth of 10 m and

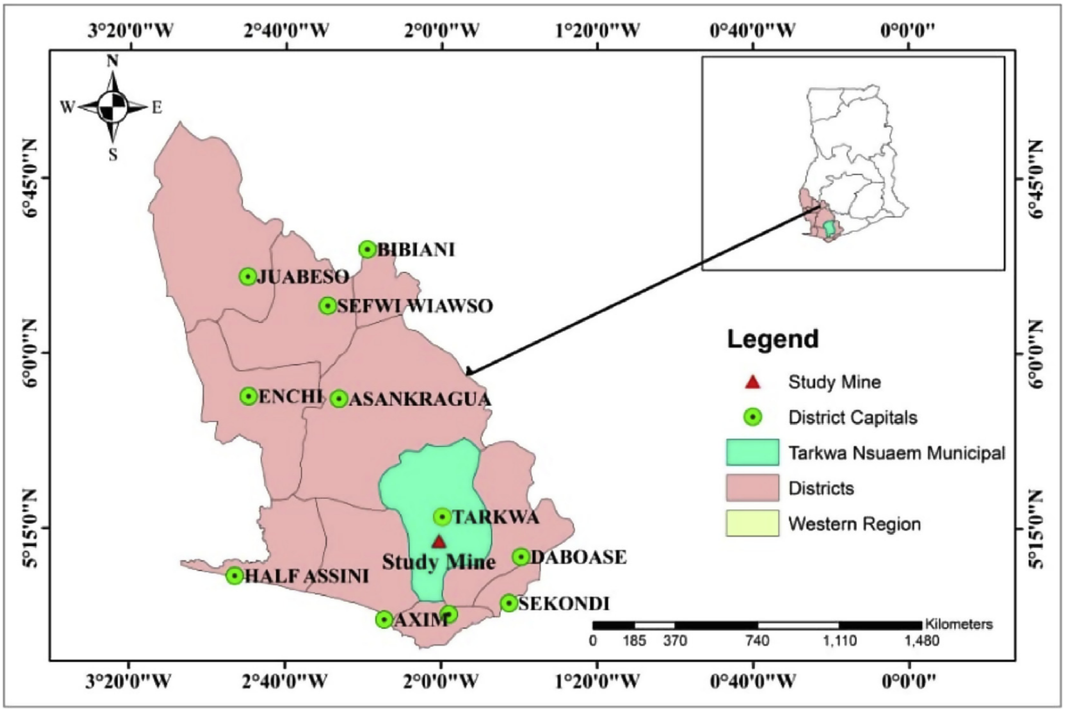

Fig. 1. Location of study area.

a sub-drill of 1 m. The drill pattern adopted by the Mine is a staggered pattern with a burden and spacing of 3.5–4 m.

In developing the various prediction models explored in this study, a dataset consisting of a total of 210 blasts, which was obtained from the surface mine in Ghana, was used. The dataset consisted of hole depth (m), maximum instantaneous charge (kg), number of blast holes, powder factor (kg/m^3) and distance from blasting point to the monitoring station(m)as the input parameters and PPV as the output parameter for the development of the proposed WNN as well as BPNN, RBFNN, GRNN, GMDH models. In the selection of the input parameters for the modelling, consideration was given to the scientific research works which indicate the influence of these parameters on blast-induced ground vibration (Hasanipanah et al., 2015; Hasanipanah et al., 2018 and references therein). For the conventional empirical techniques, the distance from the blasting point to the monitoring station (m) and maximum instantaneous charge (kg) are the required inputs for determining the model. The statistical ranges of the various input and output parameters used are outlined in Table 1. It is noteworthy that the values for hole depth (m), maximum instantaneous charge (kg), number of blast holes, powder factor (kg/m^3) were acquired from the blasting plans. Global positioning system (GPS) was used to compute the values for the distance from the blasting point to the monitoring stations. This was done by recording the coordinates between the monitoring station and the blasting point for each blast. A 3000 EZ plus portable seismic monitor that has a geophone was used to observe and measure the PPV values. The seismic monitor was setup by fixing the geophone on stable and levelground. It is worth noting that ground vibration monitoring was performed next to the building closest to the mining pit in the closest area of settlement.

The entire dataset of 210 blasts was divided into two separate sets (training and testing). The training data used to build the predictive model comprised of 130 blast data events. The 80 pieces of blast data left was then used to test the efficiency of the trained predictive model. In this study, the most widely and successfully used data division technique that has been applied throughout blast-induced ground vibration prediction studies known as the hold-out cross-validation was adopted (Monjezi et al., 2016; Ghoraba et al., 2016; Armaghani et al., 2016; Faradonbeh et al., 2016b; Hasanipanah et al., 2017a; Hasanipanah et al., 2017b; Hasanipanah et al., 2017c; Shahnazar et al., 2017; Taheri et al., 2017; Hasanipanah et al., 2018 and references therein). In the hold-out cross-validation approach the general rule is that for soft computing methods to give good predictions the sample size of the training data must be larger than the testing data and should represent the entire characteristic features of the dataset. Therefore, to meet the hold-out cross-validation condition, the training and testing data must be selected purposively and the training and testing data points for the modelling must have very closely related statistical properties that represent the same population. This is necessary because if the range of testing data is completely outside the training data range, there is the likelihood of experiencing overfitting. Therefore, the selection of the 130 pieces of data to build the model and the 80 for testing was based on the aforementioned elaborated principles.

Table 1
Statistical description of the dataset.

Parameters	Unit	Minimum	Maximum	Average	Standard deviation
Number of blast holes	-	19	355	122.50	52.37
Maximum instantaneous charge	kg	11.60	123.49	90.08	19.54
Distance from blasting point	m	573	1500	915.01	234.62
Hole depth	m	3.73	12.58	10.45	1.14
Powder factor	kg/m^3	0.10	0.97	0.69	0.15
Peak Particle Velocity	mm/s	0.13	1.65	0.79	0.32

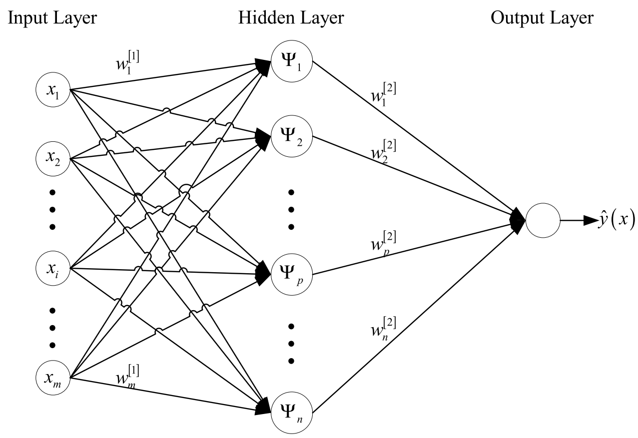

Fig. 2. WNN architecture.

3. Research methodology

In this section, a brief conceptual introduction of all the models (BPNN, RBFNN, GRNN, WNN, GMDH and empirical techniques) used in this study is provided.

3.1. Soft computing techniques

3.1.1. Wavelet neural network

WNN as proposed by Zhang and Benvenite (1992) is a new class of neural network for solving classification and regression related problems. Its structure is made up of three layers, these being: input, hidden and output layer. Its framework was constructed based on BPNN. However, it differs from the BPNN in that, it uses wavelet function as the activation function in place of the classic sigmoid or hyperbolic function (Wang, Guo, & Duan, 2013). The structure of a WNN with output $\hat{y}(x)$, input vector $x = (x_1, x_2, ..., x_i, ..., x_m)$ and n number of mother wavelets is given in Fig. 2. The received inputs are sent to the hidden layer by weighted connections.

In the hidden layer, the inputs are processed by a set of wavelet basis functions created by translating and dilating the mother wavelet ψ. According to Alexandridis and Zapranis (2013), three mother wavelets are usually recommended. These are: Gaussian, Mexican Hat and the Morlet wavelet. The output of the hidden layer, $\Psi_{a,b}(u)$ is given in Eq. (1)

$$\Psi_{a,b}(u) = \prod_{i=1}^{n} \psi\left(\frac{u - b_i}{a_i}\right) \tag{1}$$

where u (Eq. (2)) is the weighted inputs, a and b are the dilation and translation parameters of the mother wavelet, ψ respectively

$$u = \sum_{i=1}^{m} x_i w_i^{[1]} \tag{2}$$

The output of the hidden layer is then multiplied by the connection weights between the hidden and output layer. This serves as input to the output layer. The output of the WNN, $\hat{y}(x)$ is given in Eq. (3)

$$\hat{y}(x) = \sum_{j=1}^{n} w_j^{[2]} \Psi_{a,b}(u) \tag{3}$$

It should be noted that $w_i^{[2]}$, $w_j^{[2]}$, a_i and b_i are the parameters which are adjusted during the training phase of the WNN development. During the model building process (training), each iteration aims to minimise the error between the actual output $f(x)$ and predicted output $\hat{y}(x)$ (Eq. (4)). The training algorithm which is widely employed to backpropagate in order to minimise error is the backpropagation algorithm

$$e = \frac{1}{2}(f(x) - \hat{y}(x))^2 \tag{4}$$

3.1.2. Group method of data handling

The GMDH technique, developed by Ivakhnenko (1970), is a type of feed forward neural network for modelling non-linear, unstructured and complex systems (Mofki et al., 2018). A GMDH is a multilayer network which is made up of a set of quadratic neurons that are specially structured to connect sets of input parameters with their respective target parameters. GMDH has the ability to automatically learn the underlying complex relations that dominate the system variables in order to select the optimal network structure. This results in GMDH having a great ability to generalise and approximate complex nonlinear systems. The GMDH approach is characterised by an inductive self-organising procedure used for obtaining a multi-parametric model with feasible variants. This allows the researcher to build models of complex systems without making assumptions about the internal workings. GMDH uses a multilayer network of the second order of the Kolmogorov-Gabor polynomial (Eq. (5)) to characterise the complex nonlinear relationships among a system's input and output parameters (Assaleh, Shanableh, & Kheil, 2013)

$$\hat{y} = a_0 + a_1 x_i + a_2 x_j + a_3 x_i x_j + a_4 x_i^2 + a_5 x_j^2 \tag{5}$$

here, $\hat{y}$ is the predicted output, a is the vector of the coefficient of the polynomial function, x_i and x_j are the input variables.

In model building, the number of neurons in a subsequent layer can be excessively large as the number of inputs to the preceding layer becomes large. Subsequently, a neuron selection criterion per layer based on reducing the mean square error ϵ (Eq. (6))obtained from the difference between the predicted output $\hat{y}_i$ and the observed output y_i is used to keep the network complexity feasible (Assaleh et al., 2013)

$$\varepsilon = \frac{1}{p}\sum_{k=1}^{p}(y_i - \hat{y}_i)^2 \leftarrow \min \tag{6}$$

where p denotes the entire number of samples observed.

A typical example of GMDH architecture with four inputs and 3 layers and selected and unselected neurons is shown in Fig. 3.

3.1.3. Backpropagation neural network

The BPNN, as shown in Fig. 4, is a feed forward neural network that has input, output and hidden layers. The input layer receives external input vector X_j (Eq. (7)) which is assigned to individual weights w_{ij} with a constant bias b_i. The weighted inputs are then transmitted to the hidden layer

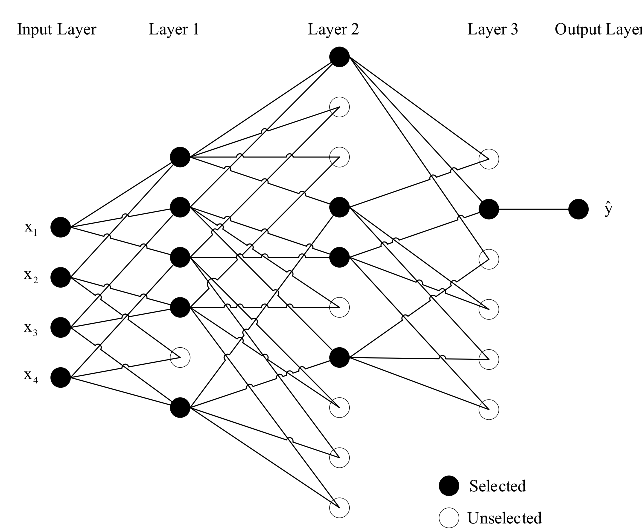

Fig. 3. GMDH architecture.

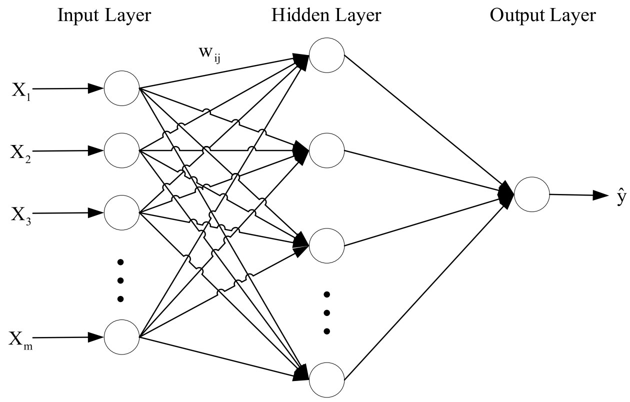

Fig. 4. BPNN architecture.

$$X_j = (X_1, X_2, X_3, \ldots, X_m)^T \tag{7}$$

The inputs to each hidden layer neuron is then transformed via a mathematical non-linear activation function. The preferred transfer function is either the hyperbolic tangent or the logarithmic sigmoid (Dorofki, Elshafie, Jaafar, Karim, & Mastura, 2012). The output from the hidden layer Y_i (Eq. (8)) is then fed as input to the output layer

$$Y_i = f\left(\sum_{j=1}^{m} (w_{ij}X_j + b_i)\right) \tag{8}$$

where w_{ij} is the weight connecting the input layer to the hidden layer, b_i denotes the bias term and f is the transfer function used in the hidden layer.

In the output layer, the input-output transformation is carried out by the linear activation function in order to produce a final network output $\hat{y}$ (Eq. (9))

$$\hat{y} = Y_i \tag{9}$$

3.1.4. Radial basis function neural network

RBFNN is a three-layered feed forward neural network made up of an input layer, a single hidden layer and an output layer. A typical example of RBFNN architecture of input vector $X_i(X_1, X_2, X_3, \ldots, X_m)$, radial basis functions $(\phi_1, \phi_2, \phi_3, \ldots, \phi_r)$, weights $(w_1, w_2, w_3, \ldots, w_r)$ and output $(\hat{y})$ is illustrated in Fig. 5. The input layer transmits inputs from the environment external to the hidden layer without any weight connections. In each hidden layer's neuron is a radial basis activation function which accounts for the non-linear processing element in the hidden layer (Shin & Park, 2000). This study applied the widely used Gaussian radial basis function. The Gaussian function responds only to a small input space region where the Gaussian is centred (Poulos, Belesiotis, & Alexandris, 2010; Singla, Subbarao, & Junkins, 2007). Each neuron then computes the Euclidean distance from each input object to the centre of the Gaussian function. Finding suitable centres for the Gaussian function is required in order to successfully implement the RBFNN. The Gaussian function is characterised by two parameters, namely: width parameter σ_j and centre c_j. The computed Euclidean norm is then sent into the Gaussian function to output net_j as shown in Eq. (10)

$$net_j = \exp\left(-\frac{\|X_i - c_j\|^2}{2\sigma_j^2}\right) \tag{10}$$

here $\|X_i - c_j\|$ denotes the computed Euclidean distance between c_j and X_i. The input to the output layer is the weighted sum of the outputs of the hidden neurons. This is then processed in the output layer by a linear function to produce the final output $\hat{y}_l$ of the RBFNN as expressed in Eq. (11)

$$\hat{y}_l = b + \sum_{j=1}^{p} w_{jl} net_j \tag{11}$$

where p is the number of neurons in the hidden layer, b is the bias term and w_{jl} denotes the weight connecting the hidden layer to the output layer.

The width parameters, centres, and the connection weights are the parameters that are adjusted in the process of training RBFNN. It is worth noting that the training is aimed at reducing the mean square error (Eq. (12)) between the predicted output y_l and the actual output a_l

$$\text{Minimise (Mean Square Error)} = \frac{1}{R}\sum_{l=1}^{R} (a_l - \hat{y}_l)^2 \tag{12}$$

where R is the number of observations.

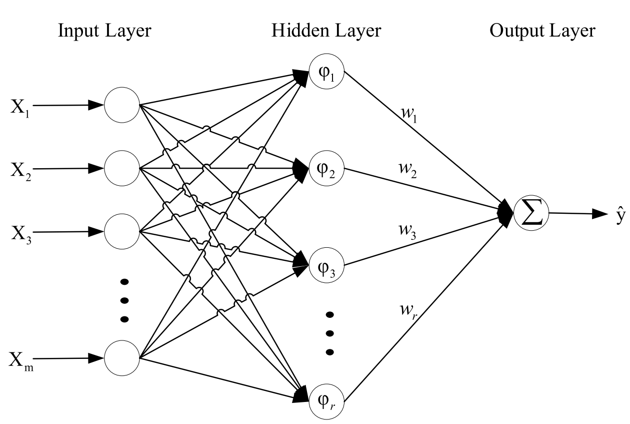

Fig. 5. RBFNN architecture.

3.1.5. Generalised regression neural network

GRNN is a feed forward neural network with a one pass learning algorithm. It is a highly parallel structure with four layers, i.e.: an input layer, pattern layer, summation layer and output layer as shown in Fig. 6 (Specht, 1991). The input layer receives data from the external environment and transmits this to the pattern layer. This pattern layer contains radial basis neurons whose transfer function is Gaussian with a spreading factor (Dong-xiao, Da, & Mian, 2008). Each radial basis neuron represents a training pattern in the pattern layer. The output of the pattern layer measures the distance from the inputs to the stored pattern. The summation layer is made up of the S-summation neuron and the D-summation neuron. Each neuron in the pattern layer is connected to these two neurons in the summation layer. The D-summation outputs a sum of the unweighted output of the pattern neurons while the S-summation outputs a summation of the weighted output. The quotient of the two outputs of the summation layer to produce the predicted value $\hat{Y}(X)$ (Eq. (13)) is finally computed by the output layer

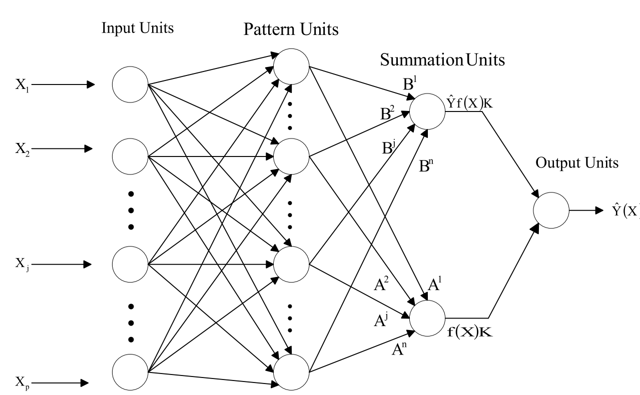

Fig. 6. GRNN architecture.

$$\hat{Y}(x) = \frac{\sum_{k=1}^{n} w_k \exp\left(-\frac{(X-X_k)^2}{2\zeta^2}\right)}{\sum_{k=1}^{n} \exp\left(-\frac{(X-X_k)^2}{2\zeta^2}\right)} \tag{13}$$

where n denotes the number of elements of the input vector, X_k and X represent the kth element of the input vector and ζ is the spread parameter.

3.2. Empirical techniques

In order to assess the performance of the previously explained ANN models, four conventional empirical models, i.e. the Indian Standard, USBM, Langefors and Kilhstrom and Ambrasey-Hendron (Ambraseys & Hendron, 1968; Duvall & Petkof, 1959; Indian Standard Institute, 1973; Langefors & Kihlstrom, 1963) were also selected and applied for comparison. These were selected, due to their widespread application (Khandelwal & Singh, 2006; Saadat et al., 2014; Mohamadnejad, Gholami, & Ataei, 2012; Armaghani, Hajihassani, Mohamad, Marto, & Noorani, 2014; Tiile, 2016; Ragam & Nimaje, 2018a and references therein) over the years as benchmark techniques to compare with soft computing techniques for blast-induced ground vibration prediction. Hence, these empirical methods were applied and compared to the WNN approach proposed in this study. Furthermore, these empirical models were applied because, currently, they are the models employed by mining companies in Ghana for the purpose of predicting ground vibration induced by blasting.

These techniques are mathematically expressed in Eqs. (14)–(17).

i. Indian Standard

$$PPV = k\left[\frac{w}{d^{2/3}}\right]^{b} \tag{14}$$

ii. USBM

$$PPV = k\left[\frac{d}{w^{1/2}}\right]^{-b} \tag{15}$$

iii. Langefors and Kilhstrom

$$PPV = k\left[\frac{w^{1/2}}{d^{3/4}}\right]^{b} \tag{16}$$

iv. Ambrasey-Hendron

$$PPV = k\left[\frac{d}{w^{1/3}}\right]^{-b} \tag{17}$$

where PPV is peak particle velocity (mm/s), w is the maximum instantaneous charge (kg), d is the distance from the blast face to the monitoring point, k and b are site specific constants. In this study, the site constants were determined by multiple regression analysis.

4. Evaluation criteria for model performance

The performance of the constructed BPNN, GMDH, RBFNN, WNN, GRNN and empirical models (Indian Standard, USBM, Ambrasey-Hendron, and Langefors and Kilhstrom) were evaluated using five statistical measures. These being: the coefficient of determination (R^2), root mean square error (RMSE), mean square error (MSE), correlation coefficient (R) and relative root mean square error (RRMSE).They are mathematically expressed in Eqs. (18)–(22). The MSE was used as the error criterion for determining the optimum structures of the ANN techniques utilised in this study. These selected performance indices are important as they help with the selection of a better model. The reason for this is that a model with higher R^2 and R values is better than that with lower R^2 and R values. A model with lower MSE, RMSE and RRMSE values is better than one with higher MSE, RMSE and RRMSE values.

$$R^2 = \frac{\left(\sum_{i=1}^{m}(y_i - y_{av})(\hat{y}_i - \hat{y}_{av})\right)^2}{\sum_{i=1}^{m}(y_i - y_{av})^2 \sum_{i=1}^{m}(\hat{y}_i - \hat{y}_{av})^2} \tag{18}$$

$$R = \frac{\sum_{i=1}^{m}(y_i - y_{av})(\hat{y}_i - \hat{y}_{av})}{\sqrt{\sum_{i=1}^{m}(y_i - y_{av})^2}\sqrt{\sum_{i=1}^{m}(\hat{y}_i - \hat{y}_{av})^2}} \tag{19}$$

$$MSE = \frac{1}{m}\sum_{i=1}^{m}(y_i - \hat{y}_i)^2 \tag{20}$$

$$RMSE = \sqrt{\frac{1}{m}\sum_{i=1}^{m}(y_i - \hat{y}_i)^2} \tag{21}$$

$$RRMSE = \frac{RMSE}{y_{av}} = \frac{\sqrt{\frac{1}{m}\sum_{i=1}^{m}(y_i - \hat{y}_i)^2}}{y_{av}} \tag{22}$$

here, $\hat{y}_{av}$ is the average of the predicted values, $\hat{y}_i$ is the predicted values, m denotes the total number of testing dataset, y_{av} is the average of the measured values and y_i is the measured values.

5. Results and discussion

The various models are presented in this section. The computed statistical performance criteria for the various models are also provided and discussed.

5.1. Models formed

5.1.1. Soft computing techniques

The optimal training and testing results based on the MSE and R criteria, as well as the optimal adjustable parameters that led to the development of the various soft computing models, are presented in Table 2.

The various soft computing models formed can, therefore, be described with reference to Table 2. In the development of the WNN, a Mexican hat wavelet function (Mi, Ren, Ouyang, Wei, & Ma, 2005) was used as the activation function in the hidden layer. This is because, in comparison with the other mother wavelet functions, the Mexican hat

Table 2
Optimal training and testing of R and MSE results for the various soft computing techniques.

Model	Adjustable parameters			Training		Testing	
	Width parameter	Number of neurons	Number of wavelons	R	MSE	R	MSE
WNN	-	-	3	0.9103	0.0206	0.8438	0.0227
GMDH	-	1	-	0.9049	0.0218	0.827	0.0249
BPNN	-	1	-	0.909	0.0209	0.8537	0.0217
RBFNN	1.7	9	-	0.91043	0.02059	0.84764	0.02227
GRNN	0.4	-	-	0.90977	0.02303	0.80121	0.03006

Table 3
Formulated models of the empirical equations.

Empirical Methods	Equations
Indian Standard	$PPV = 0.7676\left[\frac{w}{d^{2/3}}\right]^{0.938}$
USBM	$PPV = 300.7\left[\frac{d}{w^{1/2}}\right]^{-1.319}$
Langefors and Kihlstrom	$PPV = 61.406\left[\frac{w^{1/2}}{d^{3/4}}\right]^{1.5475}$
Ambrasey-Hendron	$PPV = 1724.4\left[\frac{d}{w^{1/3}}\right]^{-1.464}$

has been shown in previous studies to be computationally efficient and can be differentiated analytically (Jiang & Adeli, 2005). In the WNN formulation, five inputs (maximum instantaneous charge (kg), number of blast holes, powder factor (kg/m^3), hole depth (m) and distance from blasting point to monitoring station (m) and one output (PPV) were used as the input and output pattern to the WNN. The optimum number of wavelons in the hidden layer was estimated by experimenting 1 to 20 wavelons. The experimentation results revealed that, three wavelons gave the highest R and the lowest MSE based on the testing data results. The optimum WNN structure was [5–3 – 1], that is five inputs, three wavelons in the hidden layer with one output.

The developed GMDH model with the lowest MSE and highest R value was found to have three parameters in the input layer, one hidden layer with one neuron and one output. The corresponding polynomial equations of the developed GMDH for the PPV prediction are shown in Eqs. (23) and (24). In fact, these equations revealed that the main contributing input variables among the entire inputs under consideration are the powder factor (kg/m^3), the distance from blasting point to monitoring station (m), and the number of blast holes.

Layer 1

$$x_6 = 0.8228 - 0.4542(x_3) + 0.361(x_1) - 0.06975(x_1)(x_3) + 0.005446(x_3)^2 - 0.096(x_1)^2 \tag{23}$$

Output layer

$$PPV = 0.08641 + 0.731(x_6) - 0.06422(x_5) + 0.6728(x_5)(x_6) - 0.07829(x_6) - 0.04503(x_5)^2 \tag{24}$$

where x_5 is the powder factor (kg/m^3), x_3 is the distance from blasting point to the monitoring station(m), x_1 is the number of blast holes and x_6 is the result of layer 1.

The design parameters of a BPNN are the number of hidden layers to be used, type of transfer function, the training algorithm and the number of neurons in the hidden layer. This study applied a BPNN with a single hidden layer. This is because according to Hornik, Stinchcombe, and White (1989) a BPNN with one hidden layer has been found to be a universal approximator of any complex function. Furthermore, a hyperbolic tangent as well as linear transfer functions were applied in this study as the activation functions in the hidden and output layers, respectively. The Levenberg-Marquardt algorithm was utilised when training the BPNN. The training results revealed that a BPNN with one neuron in the hidden layer produced the lowest MSE and the highest R. The optimum structure of the BPNN was [5–1 – 1] which is explained as five (5) input parameters, one (1) hidden neuron with one (1) output.

The development of the RBFNN is dependent on the width parameter σ, the maximum number of neurons (n) in the hidden layer and the Gaussian activation function. The design values of σ and n were determined based on the statistical error criterion. That is, the developed RBFNN gave the lowest MSE and highest Rat $n = 9$ and $\sigma = 1.7$. This resulted in an optimum RBFNN structure of [5–9 – 1] which equates to five (5) inputs, nine (9) hidden neurons and one (1) output.

The design parameter of GRNN that affects the development of its model is the width parameter of the radial basis activation function. In this study, the design value of the width parameter was also determined via a sequential trial and error approach until minimum MSE and maximum R values were recorded. The optimum GRNN model gave the best performance with a width parameter of 0.40.

From Table 2, it can be observed that the testing error for the soft computing models was very close to the training error. This indicates a good fit of these models and that the optimum models developed are devoid of any overfitting condition.

5.1.2. Empirical techniques

Using the k and b values obtained from the multiple regression analysis, the empirical models formed are presented in Table 3.

5.2. Model performance assessment

Using the testing data, the statistical performance measures of MAE, RMSE, RRMSE, R and R^2 were used as measures to evaluate the approximation capability of the fitted models. The results are shown in Table 4.

It can be observed from Table 4 that the dimensioned error statistics of the various ANN models (WNN, BPNN, RBFNN, GRNN and GMDH) collectively outperformed the empirical models in their entirety. That is, the Langefors-Kihlstrom, USBM, Indian Standard and Ambrasey-Hendron models had the worse statistical performance when taking into account the MAE, RMSE, RRMSE, R and R^2. It can also be observed that the PPV predicted by the ANN models correlated better with the actual PPV than the empirical models. This is because the ANN models (WNN, BPNN, RBFNN, GRNN and GMDH) had R values greater than 80% while the empirical models had R values below 79%. This means that the empirical models were not better correlated than the ANN models, as they had lower R values relative to the ANN models.

Comparatively, the WNN model's prediction results are satisfactory and comparable to the BPNN and RBFNN. This can be seen from studying Table 4 which confirms that the WNN had relatively smaller error indicators of MAE, RMSE, RRMSE and high R values, similar to the benchmark methods of BPNN and RBFNN. In comparison, BPNN was the best model. However, looking at the results (Table 4), it can be observed that WNN deviated by approximately 0.0024 mm/s, 0.0035 mm/s, 0.0043 mm/s, 0.0099 and 0.0168 from the BPNN model results when taking into account MAE, RMSE, RRMSE, R and R^2. Furthermore, the WNN model was able to account for 71.20% (Table 4) of the variation of the predicted PPV which was very close to that accounted for by the BPNN (72.88%) and RBFNN (71.85%). The other ANN models of GMDH and GRNN accounted for 68.70% and 68.69%of the variation, respectively. The empirical models, however, could only explain a maximum of about 61% of the variation of the predicted PPV.

Table 4
Summary performance statistics for the various models.

Various models	Performance criteria				
	MAE	RMSE	RRMSE	R	R^2
WNN	0.1240	0.1508	0.1856	0.8438	0.7120
GMDH	0.1305	0.1579	0.1943	0.8289	0.6870
BPNN	0.1216	0.1473	0.1813	0.8537	0.7288
GRNN	0.1458	0.1734	0.2134	0.8012	0.6869
RBFNN	0.1213	0.1492	0.1837	0.8476	0.7185
USBM	0.1818	0.2369	0.2916	0.7622	0.5810
Ambrasey-Hendron	0.2009	0.2566	0.3159	0.7466	0.5574
Indian Standard	0.1504	0.1849	0.2276	0.7554	0.5707
Langefors-Kihlstrom	0.1630	0.2136	0.2629	0.7833	0.6136

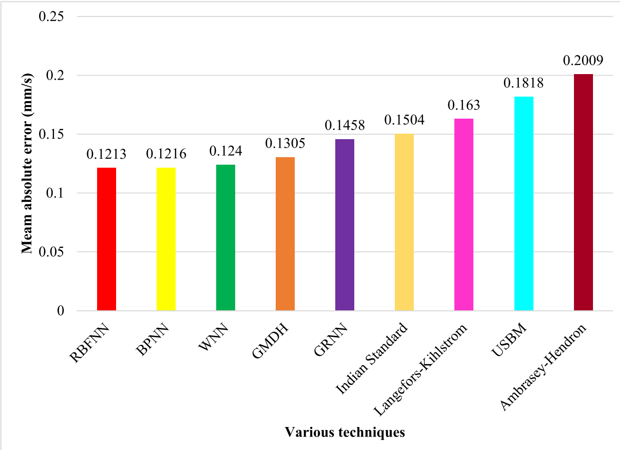

Fig. 7. Performance of various techniques using mean absolute error.

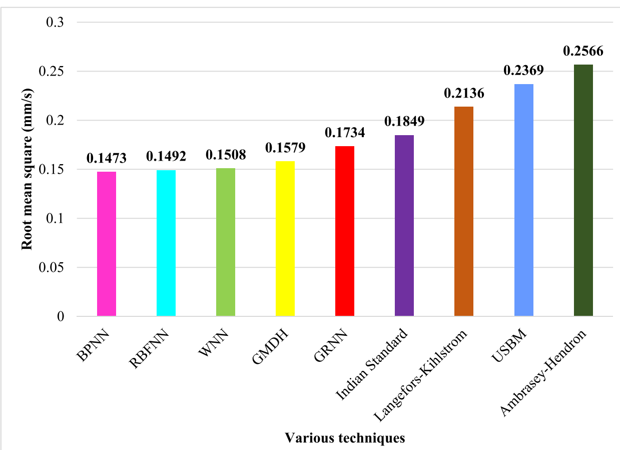

Fig. 8. Performance of various techniques using root mean square error.

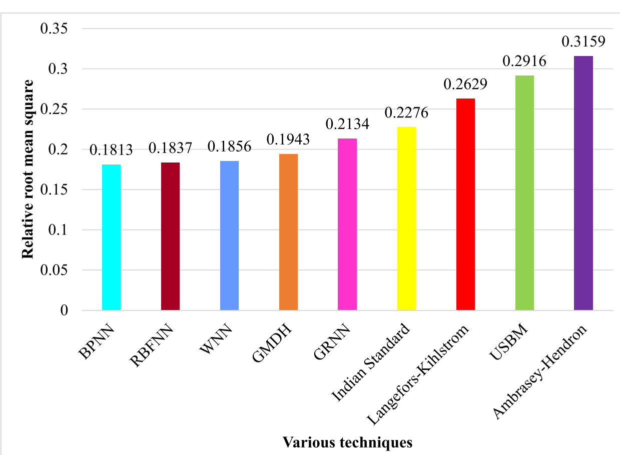

Fig. 9. Performance of various techniques using relative root mean square error.

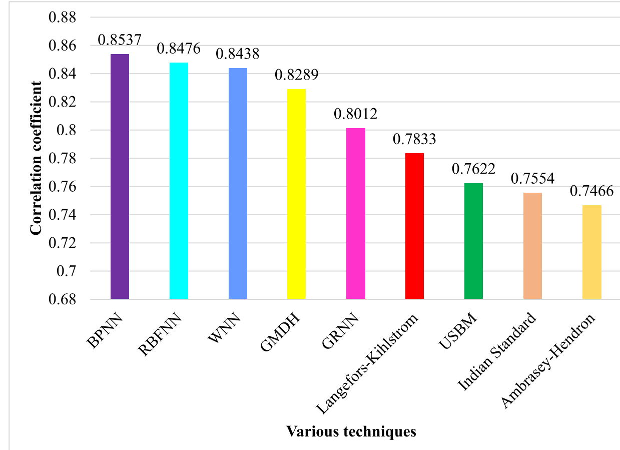

Fig. 10. Performance of various techniques using correlation coefficient.

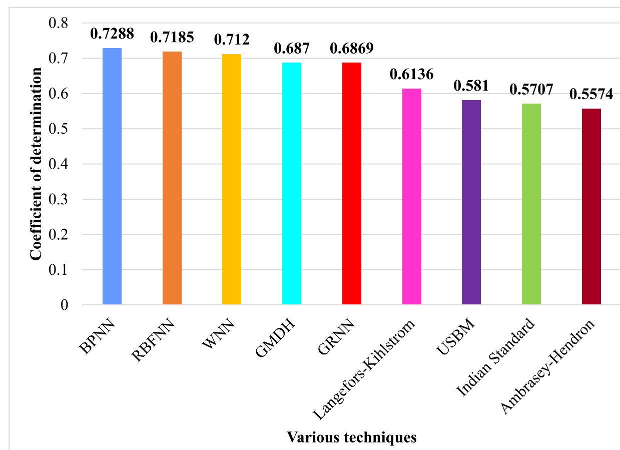

Fig. 11. Performance of various techniques using coefficient of determination.

This reveals that the observed PPV swere better replicated by the ANN models than the empirical methods. The explained results are graphically illustrated by Figs. 7–11.

The correlation between the various techniques was also calculated and presented in Table 5.

It can be observed from Table 5 that the prediction of the various ANN models (BPNN, RBFNN, WNN, GRNN and GMDH) had very strong correlation between themselves, ranging from 0.9351 to 0.9967. This indicates that PPV prediction by WNN, GMDH, GRNN, RBFNN and BPNN are almost similar. It can also be seen that the PPV predicted by the empirical models also had a correlation range of 0.8758–0.9965. In comparison, the ANN models have demonstrated superiority over conventional vibration predictors due to the fact that the ANN models in general have the ability to adequately learn and model non-linear and complex relationships in real world situations. In Table 5, it can be observed that the WNN whose efficiency was tested has demonstrated good prediction capabilities and could serve as a supplementary tool in the prediction of ground vibration induced by blasting. This assertion has been made because the correlation between the PPV predicted by WNN and the best performing model (BPNN) was 0.9891 and the correlation between the PPV predicted by WNN and RBFNN (the second best performing model) was 0.9967. These correlation results indicate the predictive accuracy and linear dependency strength of WNN and support its application for blast-induced ground vibration prediction. Mathematically, the strength of the WNN approach lies in its ability to expand and contract its basis function to detect, simultaneously, the pattern characteristics of the measured PPV. That is, the nonlinear approximation ability of WNN is augmented by the combination of the strengths of discrete wavelet transformation and neural network processing (Shen & Li, 2013).

6. Conclusions

In this study, WNN has been tested for the first time as an adaptive

Table 5
Computed correlation coefficient among the various models.

	Observed *PPV*	WNN	BPNN	RBFNN	GRNN	GMDH	USBM	Ambrasey-Hendron	Indian	Langefors
Observed PPV	1									
WNN	0.8438	1								
BPNN	0.8537	0.9891	1							
RBFNN	0.8476	0.9967	0.9892	1						
GRNN	0.8012	0.9506	0.9610	0.9511	1					
GMDH	0.8289	0.9891	0.9791	0.9852	0.9351	1				
USBM	0.7622	0.8737	0.9165	0.8782	0.9331	0.8822	1			
Ambrasey-Hendron	0.7466	0.8575	0.9005	0.8611	0.9215	0.8758	0.9953	1		
Indian	0.7554	0.8500	0.8906	0.8563	0.8888	0.8147	0.9178	0.8758	1	
Langefors	0.7708	0.8813	0.9239	0.8864	0.9370	0.8809	0.9965	0.9837	0.9478	1

computational supporting tool for PPV prediction in a mine. For comparison, four benchmark methods of ANN, namely GMDH, BPNN, GRNN and RBFNN, were applied to assess the suitability of the WNN approach. In all, a dataset consisting of 210 blastevents was obtained from a mining company in Ghana and used to develop the models. One hundred and thirty (130) pieces of blast data from the total 210 was used to construct the various models. The remaining 80 pieces of blast data were used to autonomously evaluate the models' adequacy. To formulate the model, the distance from blasting point to the monitoring station (m), the number of blast holes, the powder factor (kg/m^3), hole depth (m) and the maximum instantaneous charge (kg) were the input parameters while the PPV value was used as the output parameter. To provide a comprehensive performance evaluation, the widely used empirical techniques of USBM, Ambrasey-Hendron, Indian Standard and Langefors and Kilhstrom were applied to the blast data for comparison.

Based on the obtained statistical results, the accuracy of the WNN with a single hidden layer and three wavelons was adjudged to produce satisfactory and comparable results to the benchmark methods of BPNN and RBFNN when predicting the blast-induced ground vibration. This assertion has been made because the WNN had minor deviations of approximately 0.0024 mm/s, 0.0035 mm/s, 0.0043 mm/s, 0.0099 and 0.0168 from the best performing model of BPNN, when MAE, RMSE, RRMSE, R and R^2 were considered. The overall analysis indicates that the WNN developed model has demonstrated its suitability to serve as a supplementary ANN prediction tool due to its strong calibration power and good generalisation capabilities. Therefore, the WNN model could be replicated and applied in mining and civil engineering industries where blast operation is still used as a means of rock fragmentation.

Declaration of competing interest

None declared.

Ethical statement

Authors state that the research was conducted according to ethical standards.

Funding body

Ghana National Petroleum Corporation (GNPC).

Acknowledgments

The authors would like to thank the Ghana National Petroleum Corporation (GNPC) for providing funding to support this work through the GNPC Professorial Chair in Mining Engineering at the University of Mines and Technology (UMaT), Ghana.

References

Alexandridis, A. K., & Zapranis, A. D. (2013). Wavelet neural networks: A practical guide. *Neural Networks, 42*, 1–27.

Álvarez-Vigil, A. E., González-Nicieza, C., López Gayarre, F., & Álvarez-Fernández, M. I. (2012). Predicting blasting propagation velocity and vibration frequency using artificial neural networks. *International Journal of Rock Mechanics and Mining Sciences, 55*, 108–116.

Ambraseys, N. R., & Hendron, A. J. (1968). Dynamic behavior of rock masses. In K. Stagg, & J. Wiley (Eds.). *Rock mechanics in engineering practices* (pp. 203–207). London: Wiley.

Amegbey, N., & Afum, B. O. (2015). Blast impact prediction studies at Ghana manganese company (GMC) Ltd, Nsuta, Ghana. *Ghana Mining Journal, 15*(1), 73–77.

Amnieh, B. H., Mozdianfard, M. R., & Siamaki, A. (2010). Predicting of blasting vibrations in Sarcheshmeh copper mine by neural network. *Safety Science, 38*, 319–325.

Armaghani, D. J., Hajihassani, M., Mohamad, E. T., Marto, A., & Noorani, S. A. (2014). Blasting-induced flyrock and ground vibration prediction through an expert artificial neural network based on particle swarm optimization. *Arabian Journal of Geosciences, 7*(12), 5383–5396.

Armaghani, D. J., Hajihassani, M., Sohaei, H., Mohamad, E. T., Marto, A., Motaghedi, H., et al. (2015a). Neuro-fuzzy technique to predict air-overpressure induced by blasting. *Arabian Journal of Geosciences, 8*(12), 10937–10950.

Armaghani, D. J., Hasanipanah, M., Amnieh, H. B., & Mohamad, E. T. (2018). Feasibility of ICA in approximating ground vibration resulting from mine blasting. *Neural Computing & Applications, 29*(9), 457–465.

Armaghani, D. J., Mohamad, E. T., Hajihassani, M., Abad, S. A. N. K., Marto, A., & Moghaddam, M. R. (2016). Evaluation and prediction of flyrock resulting from blasting operations using empirical and computational methods. *Engineering with Computers, 32*(1), 109–121.

Armaghani, D. J., Momeni, E., Abad, S. V. A. N. K., & Khandelwal, M. (2015b). Feasibility of ANFIS model for prediction of ground vibrations resulting from quarry blasting. *Environmental Earth Sciences, 74*(4), 2845–2860.

Armstrong, L. W. (2001). *Evaluation of parameters effecting blast induced vibrations*Doctoral dissertation. New South Wales: University of Wollongong.

Assaleh, K., Shanableh, T., & Kheil, Y. A. (2013). Group method of data handling for modeling magnetorheological dampers. *Intelligent Control and Automation, 4*(1), 70–79.

Davies, B., Farmer, I. W., & Attewell, P. B. (1964). Ground vibration from shallow subsurface blasts. *Engineer, 217*, 553–559.

Dehghani, H., & Ataee-pour, M. (2011). Development of a model to predict peak particle velocity in a blasting operation. *International Journal of Rock Mechanics and Mining Sciences, 48*(1), 51–58.

Dong-xiao, N., Da, L., & Mian, X. (2008). Electricity price forecasting using generalized regression neural network based on principal components analysis. *Journal of Central South University of Technology, 15*(2), 316–320.

Dorofki, M., Elshafie, A. H., Jaafar, O., Karim, O. A., & Mastura, S. (2012). Comparison of artificial neural network transfer functions abilities to simulate extreme runoff data. *2012 international conference on environment, energy and biotechnology: Vol. 33*, (pp. 39–44). Singapore: IACSIT Press.

Duvall, W. I., & Petkof, B. (1959). *Spherical propagation of explosion generated strain pulses in rock.* Washington, DC: Bureau of Mines.

Faradonbeh, R. S., Armaghani, D. J., Majid, M. A., Tahir, M. M., Murlidhar, B. R., Monjezi, M., et al. (2016a). Prediction of ground vibration due to quarry blasting based on gene expression programming: A new model for peak particle velocity prediction. *International journal of Environmental Science and Technology, 13*(6), 1453–1464.

Faradonbeh, R. S., Armaghani, D. J., Monjezi, M., & Mohamad, E. T. (2016b). Genetic programming and gene expression programming for flyrock assessment due to mine blasting. *International Journal of Rock Mechanics and Mining Sciences, 88*, 254–264.

Fengqi, H., & Lijuan, S. (2015). Wavelet neural network in the design and application of hydrological forecast. *2015 international conference on intelligent transportation, big data and smart city* (pp. 1004–1006). Halong Bay, Vietnam: IEEE.

Ghasemi, E., Ataei, M., & Hashemolhosseini, H. (2013). Development of a fuzzy model for predicting ground vibration caused by rock blasting in surface mining. *Journal of Vibration and Control, 19*(5), 755–770.

Ghasemi, M. R., & Ghorbani, A. (2007). Application of wavelet neural networks in optimization of skeletal buildings under frequency constraints. *International Journal of Intelligent Technology, 2*(4), 223–231.

Ghoraba, S., Monjezi, M., Talebi, N., Armaghani, D. J., & Moghaddam, M. R. (2016). Estimation of ground vibration produced by blasting operations through intelligent and empirical models. *Environmental Earth Sciences, 75*(15), 1137.
Ghosh, A., & Daemen, J. K. (1983). A simple new blast vibration predictor (based on wave propagation laws). *The 24th US symposium on rock mechanics* (pp. 151–161). Texas, USA: American Rock Mechanics Association.
Görgülü, K., Arpaz, E., Demirci, A., Koçaslan, A., Dilmaç, M. K., & Yüksek, A. G. (2013). Investigation of blast-induced ground vibrations in the Tülü Boron open pit mine. *Bulletin of Engineering Geology and the Environment, 72*(3–4), 555–564.
Görgülü, K., Arpaz, E., Uysa, Ö., Durutürk, A. G., Yüksek, A. G., Koçaslan, A., et al. (2015). Investigation of the effects of blasting design parameters and rock properties on blast-induced ground vibrations. *Arabian Journal of Geosciences, 8*(6), 4269–4278.
Gupta, R. N., Roy, P. P., & Singh, B. (1987). On a blast induced blast vibration predictor for efficient blasting. *Proceedings of the 22nd international conference on safety in mines research Institute* (pp. 1015–1021). Beijing, China: China Coal Industry Publishing House.
Hajihassani, M., Armaghani, D. J., Marto, A., & Mohamad, E. T. (2015). Ground vibration prediction in quarry blasting through an artificial neural network optimized by imperialist competitive algorithm. *Bulletin of Engineering Geology and the Environment, 74*(3), 873–886.
Hasanipanah, M., Armaghani, D. J., Amnieh, H. B., Koopialipoor, M., & Arab, H. (2018). A risk-based technique to analyze flyrock results through rock engineering system. *Geotechnical & Geological Engineering, 36*(4), 2247–2260.
Hasanipanah, M., Faradonbeh, R. S., Amnieh, H. B., Armaghani, D. J., & Monjezi, M. (2017a). Forecasting blast-induced ground vibration developing a CART model. *Engineering with Computers, 33*(2), 307–316.
Hasanipanah, M., Golzar, S. B., Larki, I. A., Maryaki, M. Y., & Ghahremanians, T. (2017b). Estimation of blast-induced ground vibration through a soft computing framework. *Engineering with Computers, 33*(4), 951–959.
Hasanipanah, M., Monjezi, M., Shahnazar, A., Armaghani, D. J., & Farazmand, A. (2015). Feasibility of indirect determination of blast induced ground vibration based on support vector machine. *Measurement, 75*, 289–297.
Hasanipanah, M., Naderi, R., Kashir, J., Noorani, S. A., & Qaleh, A. Z. A. (2017c). Prediction of blast-produced ground vibration using particle swarm optimization. *Engineering with Computers, 33*(2), 173–179.
Hornik, K., Stinchcombe, M., & White, H. (1989). Multilayer feed forward networks are universal approximators. *Neural Networks, 2*(5), 359–366.
Hung, S. L., Huang, C. S., & Wen, C. M. (2004). Using wavelet neural network for the identification of a building structure from experimental data. *13th World Conference on Earthquake Engineering* (pp. 1–6). Vancouver, BC, Canada.
Indian Standard Institute (1973). *Criteria for safety and design of structures subject to underground blasts.* New Delhi, India: Bureau of Indian Standards.
Iramina, W. S., Sansone, E. C., Wichers, M., Wahyudi, S., Eston, S. M., Shimada, H., et al. (2018). Comparing blast-induced ground vibration models using ANN and empirical geomechanical relationships. *REM-International Engineering Journal, 71*(1), 89–95.
Ivakhnenko, A. G. (1970). Heuristic self-organization in problems of engineering cybernetics. *Automatica, 6*(2), 207–219.
Jiang, X., & Adeli, H. (2005). Dynamic wavelet neural network model for traffic flow forecasting. *Journal of Transportation Engineering, 131*(10), 771–779.
Khandelwal, M., & Singh, T. N. (2006). Prediction of blast induced ground vibrations and frequency in opencast mine: A neural network approach. *Journal of Sound and Vibration, 289*(4–5), 711–725.
Khandelwal, M., & Singh, T. N. (2007). Evaluation of blast-induced ground vibration predictors. *Soil Dynamics and Earthquake Engineering, 27*(2), 116–125.
Khandelwal, M., & Singh, T. N. (2009). Prediction of blast-induced ground vibration using artificial neural network. *International Journal of Rock Mechanics and Mining Sciences, 46*(7), 1214–1222.
Langefors, U., & Kihlstrom, B. (1963). *The modern technique of rock blasting.* New York: John Wiley and Sons.
Lapčević, R., Kostić, S., Pantović, R., & Vasović, N. (2014). Prediction of blast-induced ground motion in a copper mine. *International Journal of Rock Mechanics and Mining Sciences, 69*, 19–25.
Mi, X., Ren, H., Ouyang, Z., Wei, W., & Ma, K. (2005). The use of the Mexican Hat and the Morlet wavelets for detection of ecological patterns. *Plant Ecology, 179*(1), 1–19.
Mohamadnejad, M., Gholami, R., & Ataei, M. (2012). Comparison of intelligence science techniques and empirical methods for prediction of blasting vibrations. *Tunnelling and Underground Space Technology, 28*, 238–244.
Mohamad, E. T., Noorani, S. A., Armaghani, D. J., & Saad, R. (2012). Simulation of blasting induced ground vibration by using artificial neural network. *The Electronic Journal of Geotechnical Engineering, 17*, 2571–2584.
Mokfi, T., Shahnazar, A., Bakhshayeshi, I., Derakhsh, A. M., & Tabrizi, O. (2018). Proposing of a new soft computing-based model to predict peak particle velocity induced by blasting. *Engineering with Computers, 34*(4), 881–888.
Monjezi, M., Ahmadi, M., Sheikhan, M., Bahrami, A., & Salimi, A. R. (2010). Predicting blast-induced ground vibration using various types of neural networks. *Soil Dynamics and Earthquake Engineering, 30*(11), 1233–1236.
Monjezi, M., Baghestani, M., Faradonbeh, R. S., Saghand, M. P., & Armaghani, D. J. (2016). Modification and prediction of blast-induced ground vibrations based on both empirical and computational techniques. *Engineering with Computers, 32*(4), 717–728.
Monjezi, M., Ghafurikalajahi, M., & Bahrami, A. (2011). Prediction of blast-induced ground vibration using artificial neural networks. *Tunnelling and Underground Space Technology, 26*(1), 46–50.
Monjezi, M., Hasanipanah, M., & Khandelwal, M. (2013). Evaluation and prediction of blast-induced ground vibration at Shur River Dam, Iran, by artificial neural network. *Neural Computing & Applications, 22*(7–8), 1637–1643.
Okkan, U. (2012). Wavelet neural network model for reservoir inflow prediction. *Scientia Iranica, 19*(6), 1445–1455.
Parida, A., & Mishra, M. K. (2015). Blast vibration analysis by different predictor approaches-a comparison. *Procedia Earth and Planetary Science, 11*, 337–345.
Poulos, M., Belesiotis, V. S., & Alexandris, N. (2010). A classroom observation model fitted to stochastic and probabilistic decision systems. *IFIP international conference on artificial intelligence applications and innovations* (pp. 30–36). Berlin, Heidelberg: Springer.
Ragam, P., & Nimaje, D. S. (2018a). Evaluation and prediction of blast-induced peak particle velocity using artificial neural network: A case study. *Noise & Vibration Worldwide, 49*(3), 111–119.
Ragam, P., & Nimaje, D. S. (2018b). Estimation of ambiguous blast-induced ground vibration using intelligent models: A case study. *Noise & Vibration Worldwide, 49*(4), 147–157.
Ragam, P., & Nimaje, D. S. (2018c). Assessment of blast-induced ground vibration using different predictor approaches- a comparison. *Chemical Engineering Transactions, 66*, 487–492.
Rai, R., & Singh, T. N. (2004). A new predictor for ground vibration prediction and its comparison with other predictors. *Indian Journal of Engineering and Materials Sciences, 11*, 178–184.
Ramana, R. V., Krishna, B., Kumar, S. R., & Pandey, N. G. (2013). Monthly rainfall prediction using wavelet neural network analysis. *Water Resources Management, 27*(10), 3697–3711.
Roy, P. P. (1991). Vibration control in an opencast mine based on improved blast vibration predictors. *Mining Science and Technology, 12*(2), 157–165.
Rustan, A., Cunningham, C., Fourney, W., Simha, K. R. Y., & Spathis, A. T. (2010). *Mining and rock construction technology desk reference: Rock mechanics, drilling & blasting.* Netherlands: CRC Press/Balkema.
Saadat, M., Khandelwal, M., & Monjezi, M. (2014). An ANN-based approach to predict blast-induced ground vibration of Gol-E-Gohar iron ore mine, Iran. *Journal of Rock Mechanics and Geotechnical Engineering, 6*(1), 67–76.
Shahnazar, A., Rad, H. N., Hasanipanah, M., Tahir, M. M., Armaghani, D. J., & Ghoroqi, M. (2017). A new developed approach for the prediction of ground vibration using a hybrid PSO-optimized ANFIS-based model. *Environmental Earth Sciences, 76*(15), 527.
Shahri, A. A., & Asheghi, A. (2018). Optimized developed artificial neural network-based models to predict the blast-induced ground vibration. *Innovative Infrastructure Solutions, 3*, 1–10.
Shen, J., & Li, W. (2013). Sensitivity analysis of wavelet neural network model for short-term traffic volume prediction. *Journal of Applied Mathematics, 2013*, 1–10.
Shin, M., & Park, C. (2000). A radial basis function approach to pattern recognition and its applications. *ETRI Journal, 22*(2), 1–10.
Silva-Castro, J. J. (2012). *Blast vibration modeling using improved signature hole technique for bench blast*Doctoral dissertation. Lexington: University of Kentucky.
Singla, P., Subbarao, K., & Junkins, J. L. (2007). Direction-dependent learning approach for radial basis function networks. *IEEE Transactions on Neural Networks, 18*(1), 203–222.
Specht, D. F. (1991). A general regression neural network. *IEEE Transactions on Neural Networks, 2*(6), 568–576.
Stojadinovic, S., Zikic, M., & Pantovic, R. (2011). A new approach to blasting induced ground vibrations and damage to structures. *Acta Montanistica Slovaca, 16*(4), 344–354.
Taheri, K., Hasanipanah, M., Golzar, S. B., & Majid, M. Z. A. (2017). A hybrid artificial bee colony algorithm-artificial neural network for forecasting the blast-produced ground vibration. *Engineering with Computers, 33*(3), 689–700.
Tiile, R. N. (2016). *Artificial neural network approach to predict blast-induced ground vibration, airblast and rock fragmentation*Masters dissertation. Rolla: Missouri University of Science and Technology.
Tripathy, G. R., Shirke, R. R., & Kudale, M. D. (2016). Safety of engineered structures against blast vibrations: A case study. *Journal of Rock Mechanics and Geotechnical Engineering, 8*(2), 248–255.
Wang, W., & Ding, J. (2003). Wavelet network model and its application to the prediction of hydrology. *Nature and Science, 1*(1), 67–71.
Wang, G., Guo, L., & Duan, H. (2013). Wavelet neural network using multiple wavelet functions in target threat assessment. *Science World Journal, 2013*, 1–7.
Xue, X., & Yang, X. (2014). Predicting blast-induced ground vibration using general regression neural network. *Journal of Vibration and Control, 20*(10), 1512–1519.
Yue, Q., & Shao-hong, L. (2014). Wavelet neural network optimization algorithm based landslide displacement forecast and prediction. *Electronic Journal of Geotechnical Engineering, 19*, 17781–17787.
Zhang, Q., & Benvenite, A. (1992). Wavelet networks. *IEEE Transactions on Neural Networks, 3*(6), 889–898.
Zhou, G., Wang, C., Wang, S., & Yin, X. (2016). Gray wavelet neural network and its application in mining waste prediction. *2016 international conference on progress in informatics and computing (PIC)* (pp. 164–168). Shanghai, China: IEEE.